

# Supporting Information

## Insights in the vibrational optical activity spectra of the antibiotic vancomycin in DMSO

Roy Aerts<sup>†</sup>, Jonathan Bogaerts<sup>†</sup>, Wouter Herrebout<sup>†</sup> and Christian  
Johannessen<sup>\*†</sup>

<sup>†</sup> *Department of Chemistry, University of Antwerp, Groenenborgerlaan 171, B-2020  
Antwerp, Belgium.*

E-mail: christian.johannessen@uantwerpen.be

### Contents

<b>S1</b>	<b>Experimental Raman and ROA spectra</b>	<b>2</b>
<b>S2</b>	<b>Geometrical factors calculated conformations</b>	<b>3</b>
	S2.1 Geometries in DMSO solvent . . . . .	4
	S2.2 Geometries in water solvent . . . . .	5
<b>S3</b>	<b>Determining scaling factors</b>	<b>6</b>
<b>S4</b>	<b>Spectral overlap integrals</b>	<b>10</b>
	S4.1 Between experimental and calculated spectra: 1150-1560 cm <sup>-1</sup> . . . . .	10
	S4.2 Between experimental and calculated spectra: 1560-1750 cm <sup>-1</sup> . . . . .	11
	S4.3 Between water and DMSO as solvent . . . . .	12
	S4.4 Between DMSO calculated spectra . . . . .	13
<b>S5</b>	<b>Boltzmann-weighted spectra</b>	<b>14</b>
<b>S6</b>	<b>Estimation of the contributions of different chemical entities to the spectra</b>	<b>16</b>
<b>S7</b>	<b>Spectral effects of carbohydrate entities</b>	<b>24</b>
<b>S8</b>	<b>Spectral calculations of reoriented hydroxyl groups</b>	<b>27</b>
<b>S9</b>	<b>Explicit DMSO spectral calculations</b>	<b>29</b>

## S1 Experimental Raman and ROA spectra

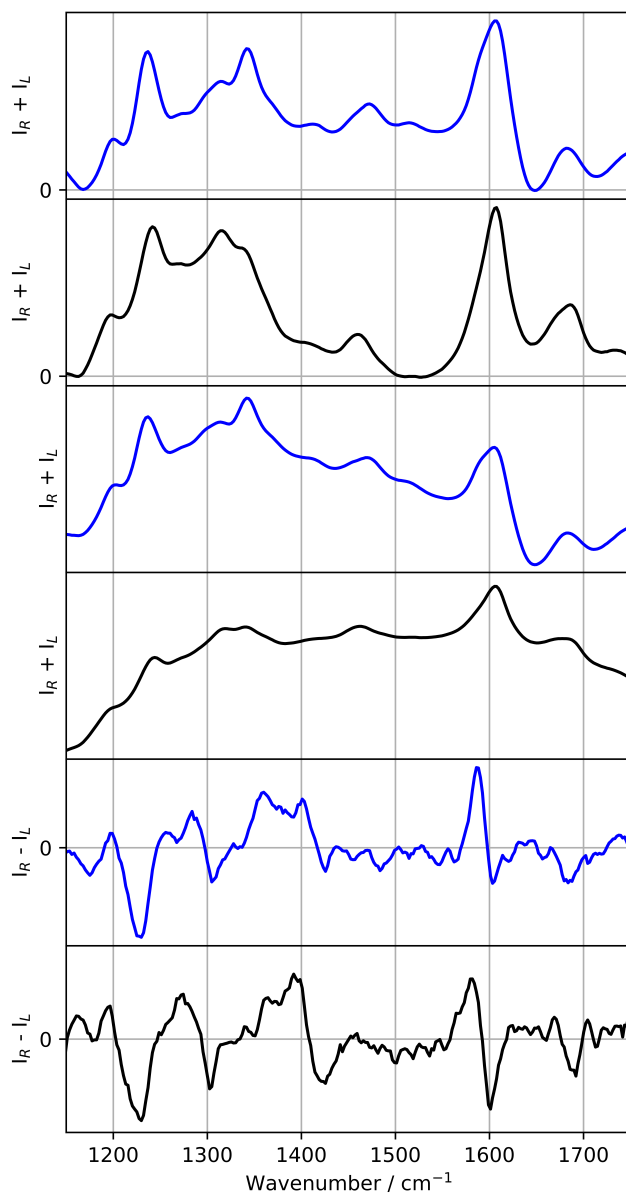


**Fig. S1** The baseline corrected (Boelens *et al.* procedure<sup>1</sup>; **A** and **B**), the non-baseline corrected Raman spectra (**C** and **D**), and the Raman optical activity spectra (**E** and **F**) of vancomycin in aqueous solution (acetate buffer, pH 3.5; blue colour) and in DMSO-d<sub>6</sub> (black colour).



## S2 Geometrical factors calculated conformations

The dihedral angles of vancomycin that are used during the analyses are shown in Fig. S2.

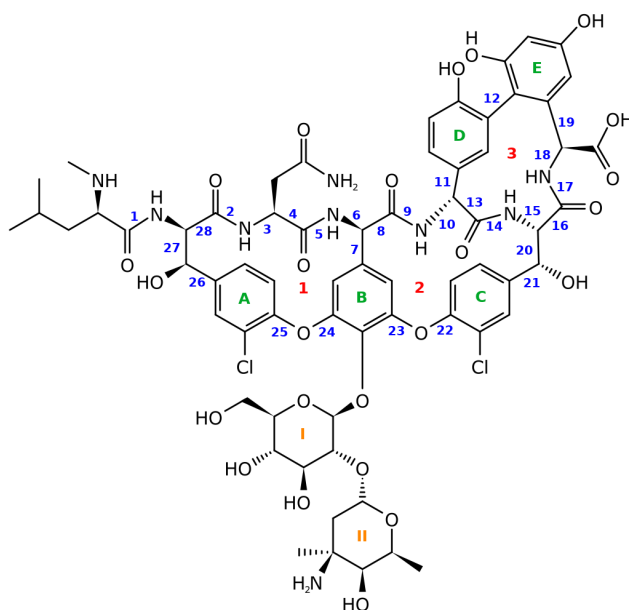


**Fig. S2** The molecular structure of vancomycin with the dihedral angles that are used for the analysis in blue.





### S3 Determining scaling factors

Prior to any quantitative comparison, the predicted spectra should be horizontally shifted to correct for the over/underestimations of the normal mode frequencies (resulting from the harmonic approximation and the use of a limited basis set). This can be done by identifying the scaling factor that maximizes the overlap integral between the experimental and predicted spectrum. The overlap integral is calculated as:

$$S_{fg} = \frac{\int f(\sigma\tilde{\nu})g(\tilde{\nu})}{\sqrt{\int f(\sigma\tilde{\nu})^2 d\tilde{\nu} \int g(\tilde{\nu})^2 d\tilde{\nu}}} \quad (1)$$

$f$  and  $g$  represent the theoretical and calculated spectra,  $\sigma$  the scaling factor for the wavenumbers of the calculated spectrum, and  $\tilde{\nu}$  the wavenumber. The overlap integral varies between 0 and 1 for Raman and -1 and 1 for ROA spectral comparisons.

If the conformation(al ensemble) of the studied molecule is known, the scaling factor can be determined based on maximizing the overlap integral between its (Boltzmann-weighted) calculated and experimental spectrum. Here, for vancomycin, we wish to start with a blank sheet: we calculate the average overlap integral between the experimental spectrum and the 55 single-conformer spectra (full curves in Fig. S5) for scaling factors between 0.950 and 1.060. This was performed using both the IR and Raman spectra in the spectral regions 1150-1560  $\text{cm}^{-1}$  and 1560-1750  $\text{cm}^{-1}$ . Additionally, as we know from previous NMR studies<sup>3,4</sup>,

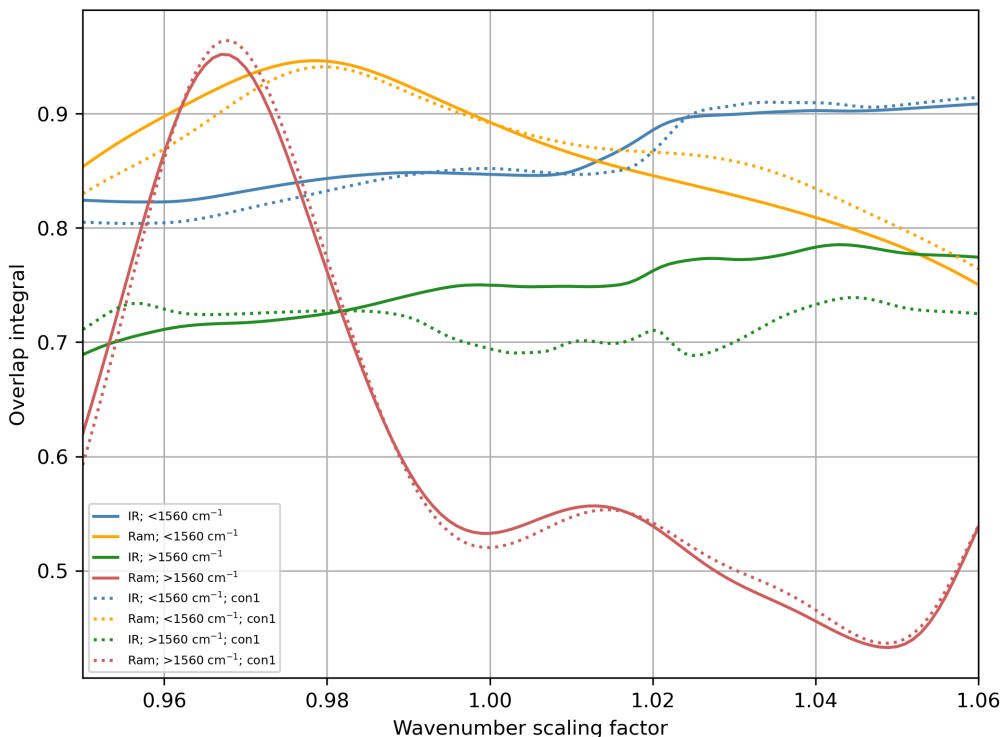


**Fig. S5** The overlap integral (calculated in different ways; see the legend in the figure) *versus* the scaling factor used on the wavenumbers of the calculated spectra.

our conformation 1 (identical to labeling in our previous work<sup>2</sup>) is the correct one and we trace its overlap integral with the experimental spectra for each scaling factor too in Fig. S5 (dashed lines; *con1* in the legend).

Usually the scaling factors for the spectral regions 1150-1560  $\text{cm}^{-1}$  and 1560-1750  $\text{cm}^{-1}$  are *grosso modo* 0.985 and 0.965, respectively.<sup>2,5</sup> Looking at the average overlap integral with respect to the applied horizontal scaling factor in the different cases, we find, based on the Raman spectra, shifts in line with the expectations (0.979 for 1150-1560  $\text{cm}^{-1}$ , 0.968 for 1560-1750  $\text{cm}^{-1}$ ). The IR spectra, on the contrary, appear not to be usable: it displays no clear maximum in the expected region and the average overlap integral does not seem to be changing as much as is the case for the Raman spectra. Why the two spectroscopies behave so differently can be rationalized from inspecting all the spectra (Fig. S6 and S7). The Raman spectra appear to be much less sensitive to the changes in conformation with respect to the IR spectra. That means that for each conformation Raman spectrum the overlap integral will maximize around the same scaling factor, making the average overlap integral react strongly on the scaling factor used. For the IR spectra the best overlap integral of each individual conformer spectrum will be highly different, resulting in a disagreement between the individual IR spectra -so to speak- when pointing out the best overlap integral. The notion behind the scaling factor is not to ensure a good overlap between the experimental spectrum and conformer spectra that are not actually present in solution, but to correct for systematic errors -identical across all conformer spectra- during the predictions of the

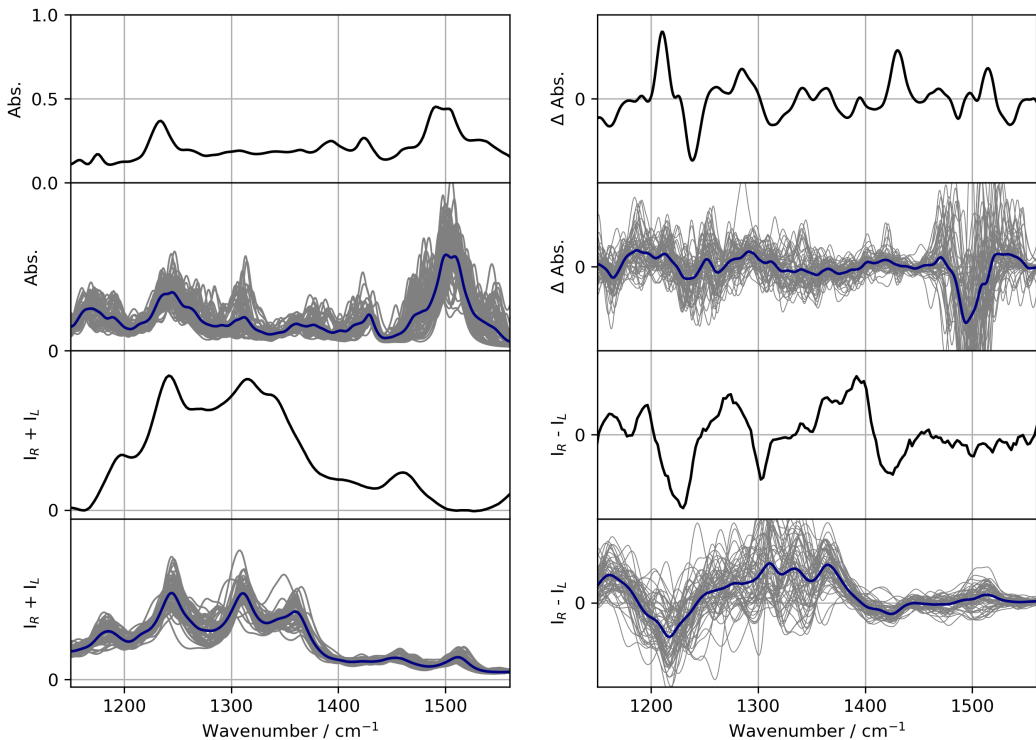


**Fig. S6** All calculated IR (top left), Raman spectra (bottom left), VCD (top right), and ROA spectra (bottom right; black: experimental, grey: single conformer calculated spectra, blue: average calculated spectrum; see main text for methodology).

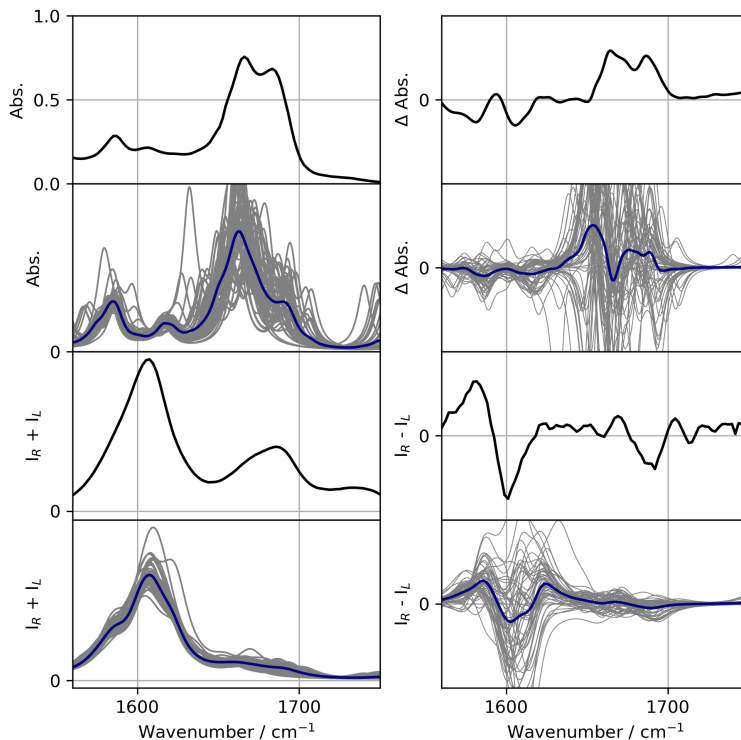


**Fig. S7** All calculated IR (top left), Raman spectra (bottom left), VCD (top right), and ROA spectra (bottom right; black: experimental, grey: single conformer calculated spectra, blue: average calculated spectrum; see main text for methodology).

frequencies. As the Raman is much less sensitive to conformational changes, using its average overlap integral is ideal for determining the scaling factor. As such, we determine a scaling factor of **0.979** for 1150-1560  $\text{cm}^{-1}$  and **0.968** for 1560-1750  $\text{cm}^{-1}$ . Of course, this correction should be identical for all spectra (IR, VCD, Raman, and ROA). This is in contrast to what we did previously for artemisinin-type products, where the scaling factor was determined based on all four spectroscopies.<sup>6</sup> For the sake of completeness we add a similar figure as **S5** for VCD and ROA (Fig. **S8**).

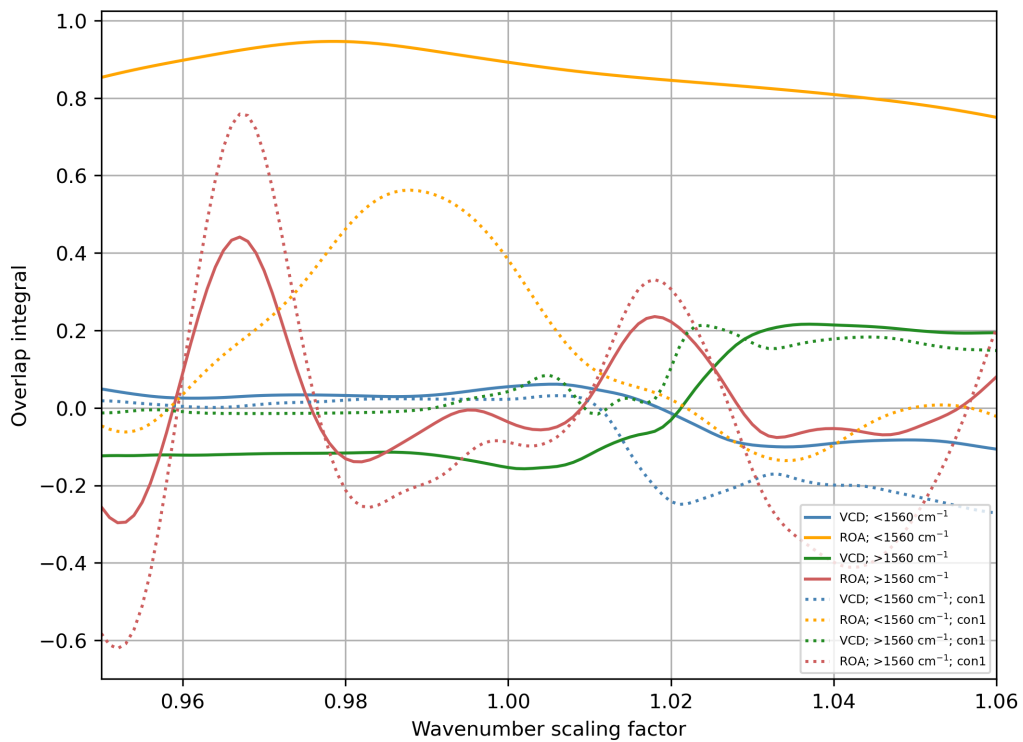


**Fig. S8** The overlap integral (calculated in different ways; see the legend in the figure) *versus* the scaling factor used on the wavenumbers of the calculated spectra.

## S4 Spectral overlap integrals

All reported overlap integrals were calculated according to equation 1. There are 55 conformations of vancomycin that are used for spectral predictions, adopted from our previous work<sup>2</sup>. The scaling factors that have been used during the overlap integral calculations were determined as elaborated in section S3.

### S4.1 Between experimental and calculated spectra: 1150-1560 $\text{cm}^{-1}$

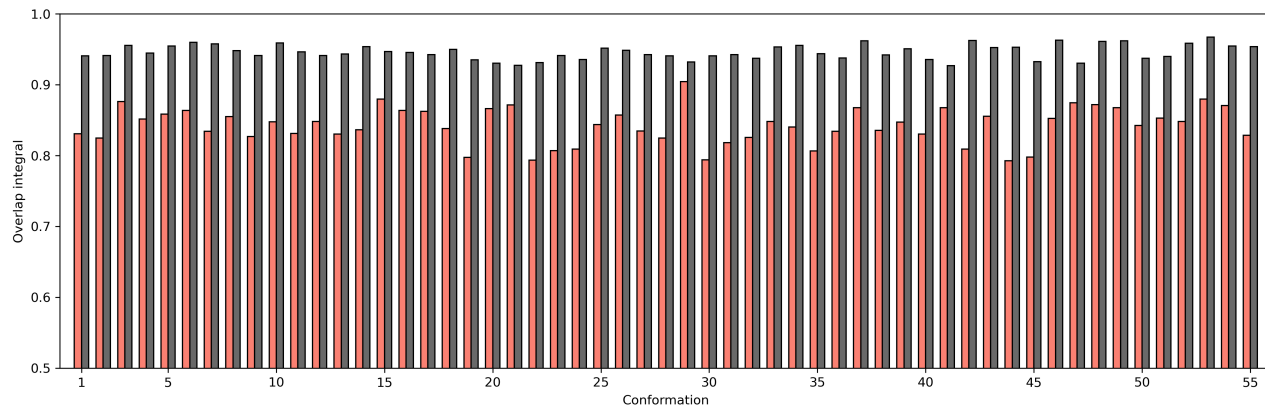


**Fig. S9** The overlap integral between the experimental Raman (grey) and IR (red) on the one hand, and each of the calculated single-conformer spectra on the other hand (spectral region 1150-1560  $\text{cm}^{-1}$ ). A scaling factor of 0.979 was applied to vertically scale the calculated spectra (see section S3).



## S4.2 Between experimental and calculated spectra: 1560-1750 $\text{cm}^{-1}$

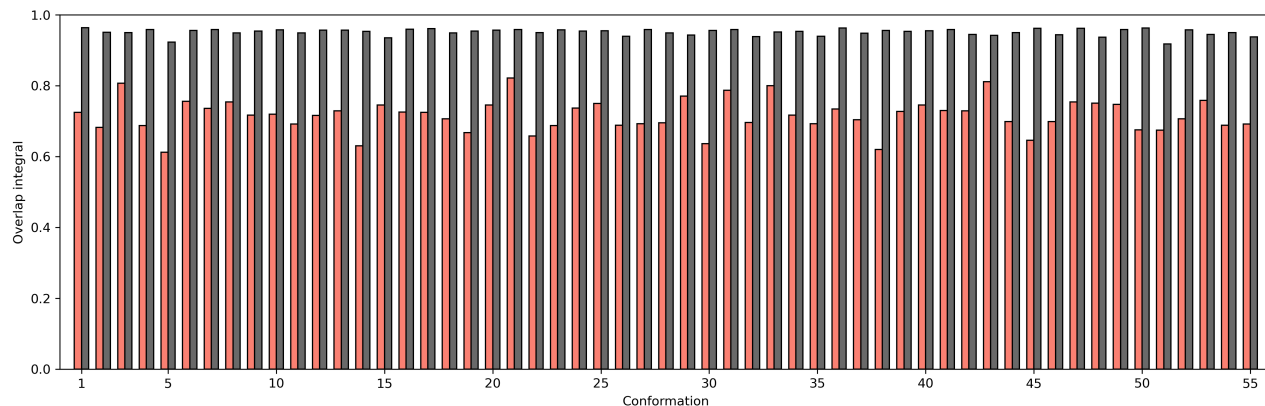


**Fig. S10** The overlap integral between the experimental Raman (grey) and IR (red) on the one hand, and each of the calculated single-conformer spectra on the other hand (spectral region 1560-1750  $\text{cm}^{-1}$ ). A scaling factor of 0.968 was applied to vertically scale the calculated spectra (see section S3).

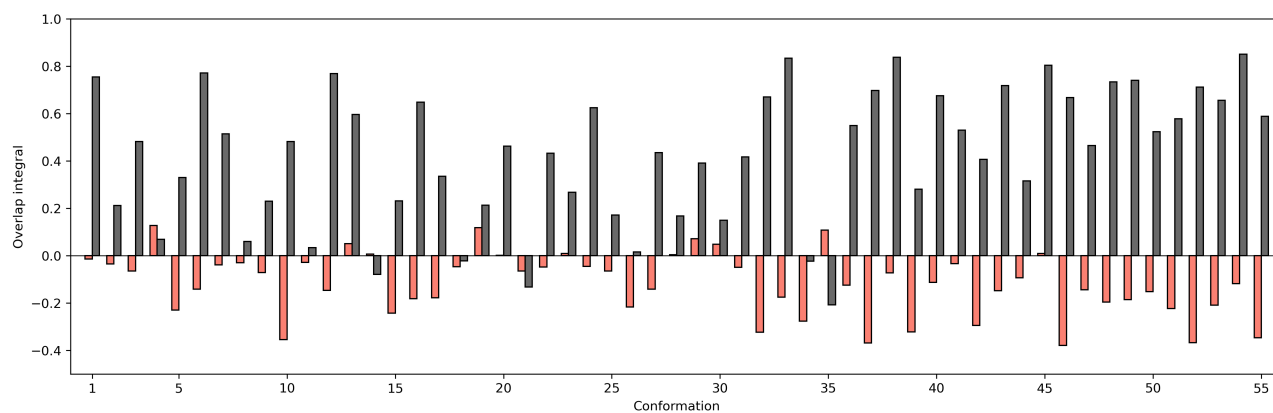


**Fig. S11** The overlap integral between the experimental ROA (grey) and VCD (red) on the one hand, and each of the calculated single-conformer spectra on the other hand (spectral region 1560-1750  $\text{cm}^{-1}$ ). A scaling factor of 0.968 was applied to vertically scale the calculated spectra (see section S3).

### S4.3 Between water and DMSO as solvent

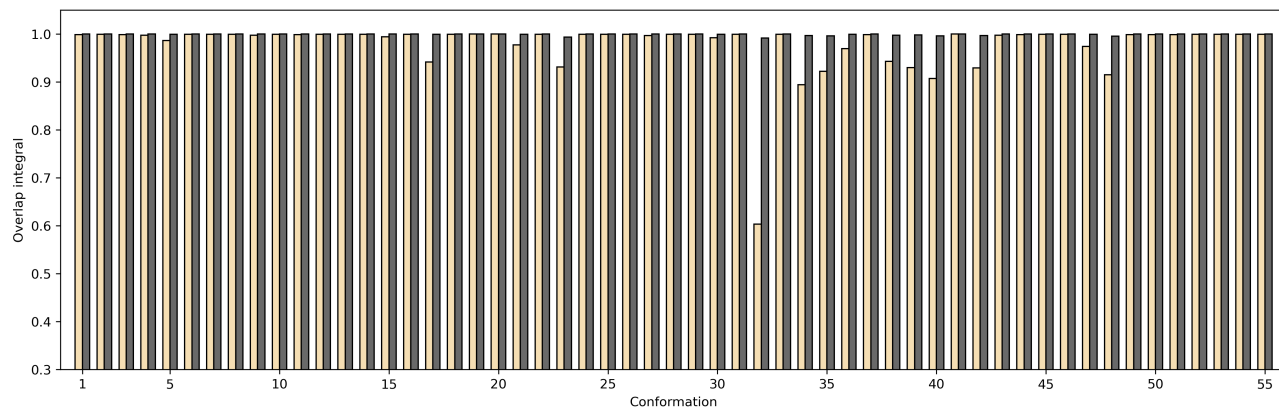


**Fig. S12** The overlap integral between the calculated Raman (grey) and ROA (lightbrown) in water and DMSO for each of the 55 conformations (spectral region  $1150-1560\text{ cm}^{-1}$ ).

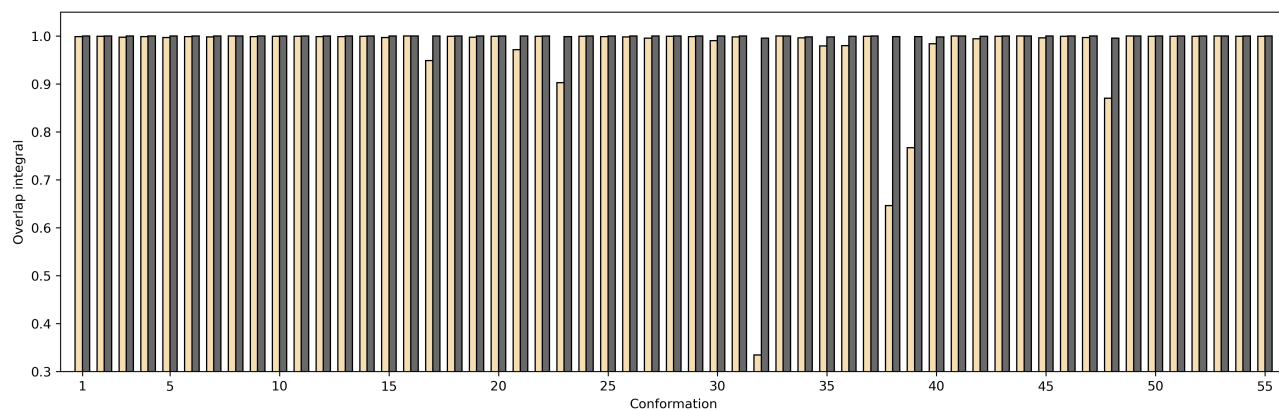


**Fig. S13** The overlap integral between the calculated Raman (grey) and ROA (lightbrown) in water and DMSO for each of the 55 conformations (spectral region  $1560-1750\text{ cm}^{-1}$ ).

## S4.4 Between DMSO calculated spectra

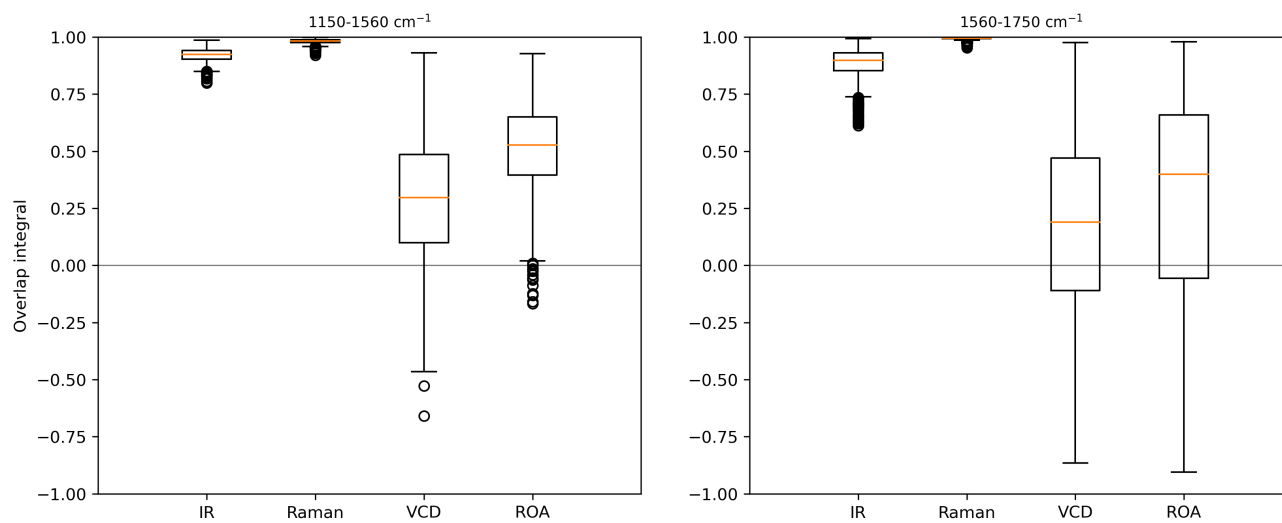


**Fig. S14** Boxplots of the  $S_{fg}$  values calculated mutually between all 55 single-conformer spectra ( $55^2 - 55/2 = 1485$   $S_{fg}$  values) for IR, Raman, vibrational circular dichroism (VCD), and Raman optical activity (ROA) in the two spectral regions  $1150\text{-}1560\text{ cm}^{-1}$  and  $1560\text{-}1750\text{ cm}^{-1}$ .

## S5 Boltzmann-weighted spectra

**Table S1** The relative enthalpies and corresponding Boltzmann weights of the conformations that contribute more than 0.5% to the Boltzmann-weighted spectrum.

Conformation	$H^\circ / \text{kcal.mol}^{-1}$	$\Delta H^\circ / \text{kcal.mol}^{-1}$	Boltzmann weight / %
31	-3624310.16	0.00	93.4
50	-3624308.51	1.65	5.8
38	-3624307.17	2.99	0.6

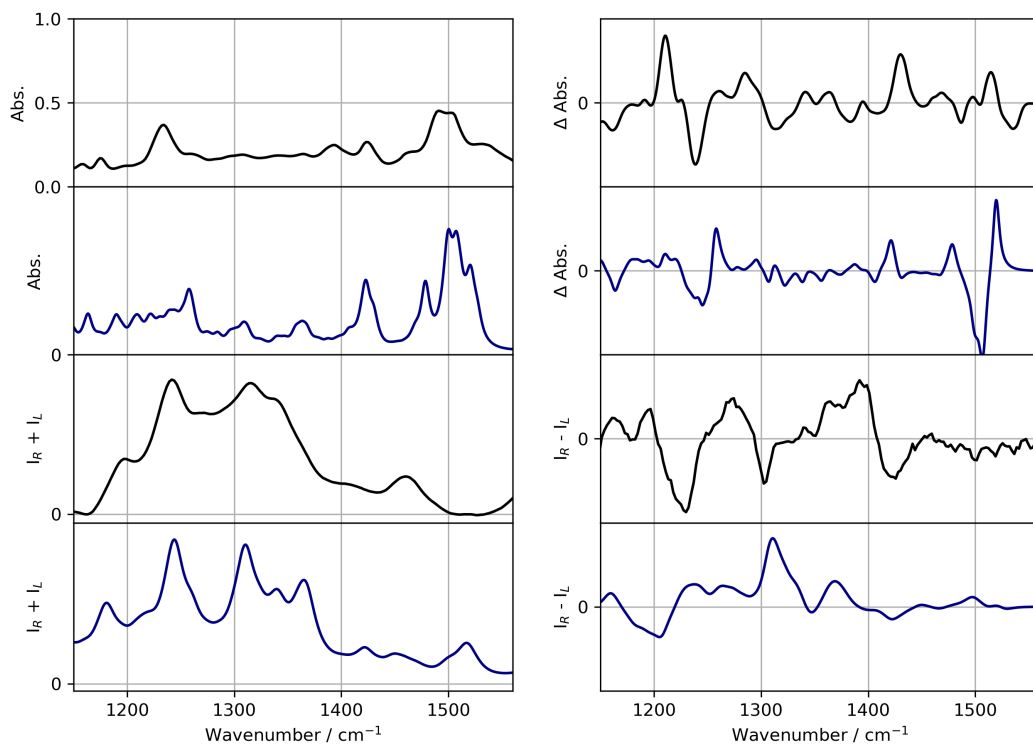


**Fig. S15** The experimental (black) and Boltzmann-weighted (blue) IR (top left), Raman (bottom left), VCD (top right), and ROA (bottom right) spectra in the 1150-1560  $\text{cm}^{-1}$  spectral region.

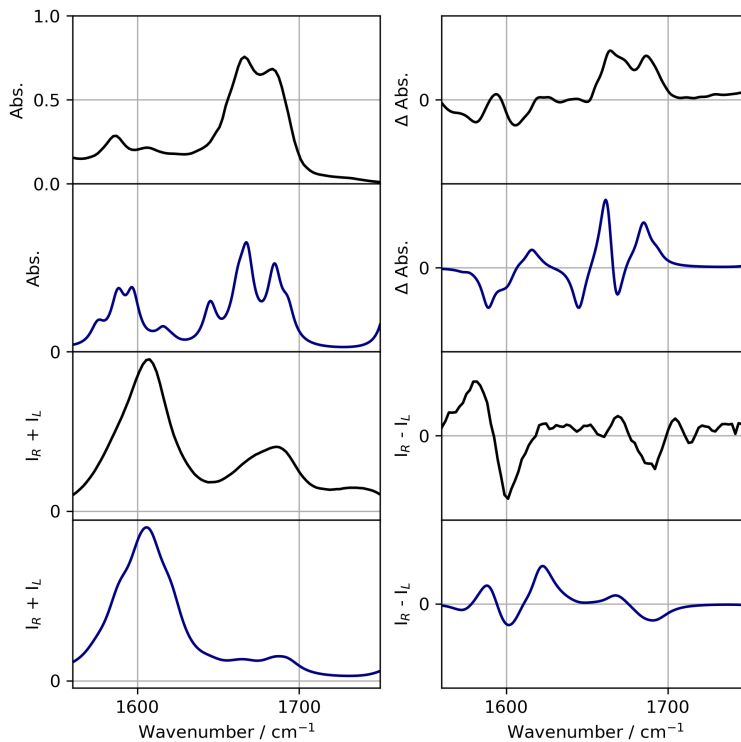


**Fig. S16** The experimental (black) and Boltzmann-weighted (blue) IR (top left), Raman (bottom left), VCD (top right), and ROA (bottom right) spectra in the 1560-1750  $\text{cm}^{-1}$  spectral region.

**Table S2** The overlap integrals between the experimental and Boltzmann-weighted spectra. The concerned spectra are given in Fig. S15 and S16.

Spec. Region / $\text{cm}^{-1}$	IR	Raman	VCD	ROA
1150-1560	0.82	0.94	0.05	-0.02
1560-1750	0.79	0.96	-0.06	0.49

## S6 Estimation of the contributions of different chemical entities to the spectra

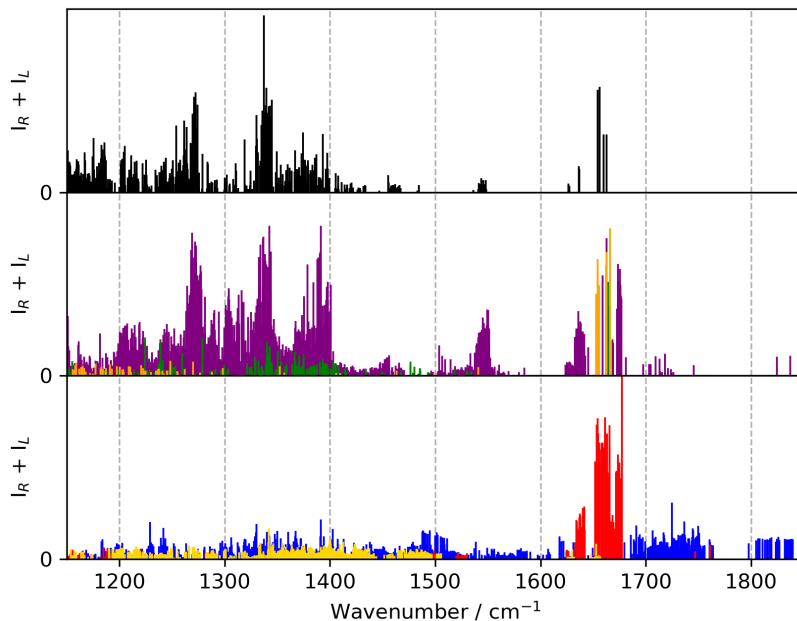


**Fig. S17** The assignment of each normal mode of all 55 conformations (with their corresponding Raman intensity) to one of the following categories: peptide+aromat+sugar (black; top), peptide+aromat (purple; middle), peptide+sugar (green; middle), aromat+sugar (orange; middle), peptide (blue; bottom), aromat (red; bottom), sugar (yellow; bottom). How this was performed is explained in our previous work<sup>2</sup>. No scaling factor was applied to the normal mode wavenumbers.

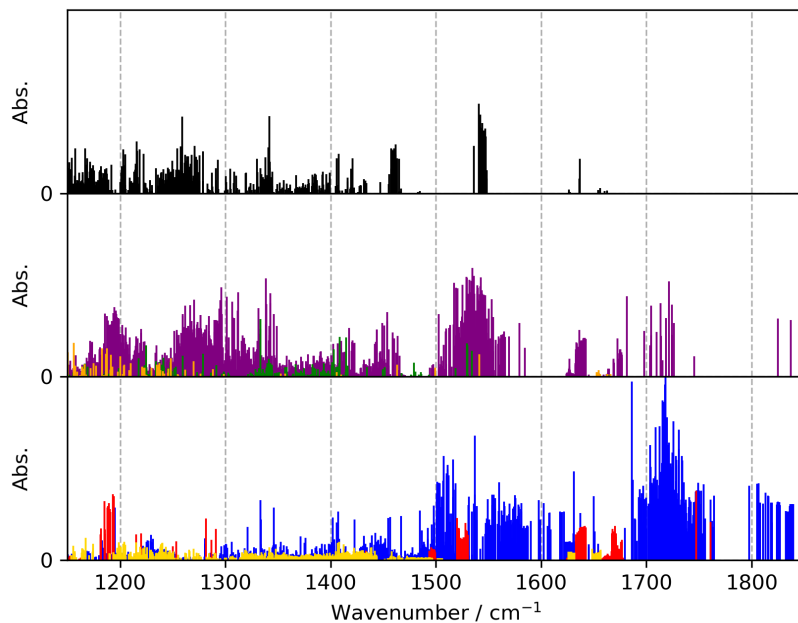


**Fig. S18** The assignment of each normal mode of all 55 conformations (with their corresponding IR intensity) to one of the following categories: peptide+aromat+sugar (black; top), peptide+aromat (purple; middle), peptide+sugar (green; middle), aromat+sugar (orange; middle), peptide (blue; bottom), aromat (red; bottom), sugar (yellow; bottom). How this was performed is explained in our previous work<sup>2</sup>. No scaling factor was applied to the normal mode wavenumbers.

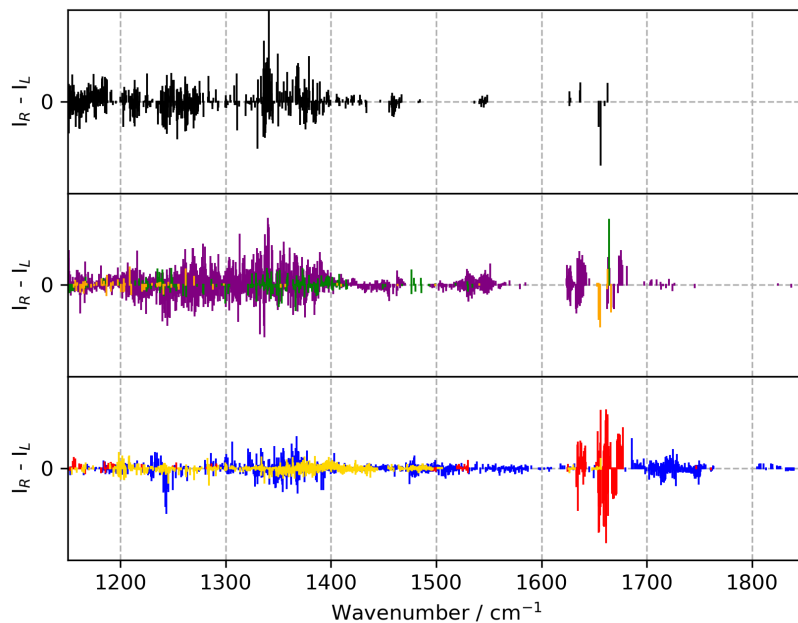


**Fig. S19** The assignment of each normal mode of all 55 conformations (with their corresponding Raman optical activity intensity) to one of the following categories: peptide+aromat+sugar (black; top), peptide+aromat (purple; middle), peptide+sugar (green; middle), aromat+sugar (orange; middle), peptide (blue; bottom), aromat (red; bottom), sugar (yellow; bottom). How this was performed is explained in our previous work<sup>2</sup>. No scaling factor was applied to the normal mode wavenumbers.



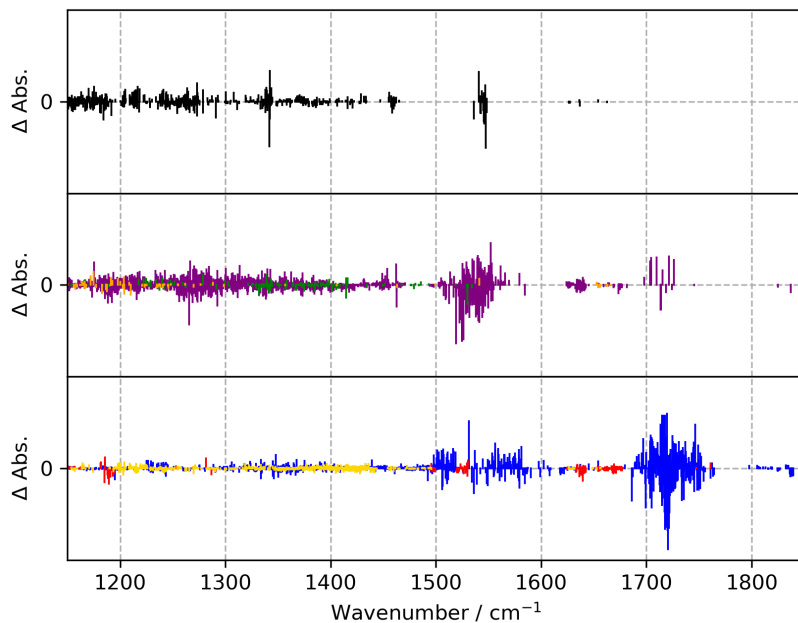


**Fig. S20** The assignment of each normal mode of all 55 conformations (with their corresponding vibrational circular dichroism intensity) to one of the following categories: peptide+aromat+sugar (black; top), peptide+aromat (purple; middle), peptide+sugar (green; middle), aromat+sugar (orange; middle), peptide (blue; bottom), aromat (red; bottom), sugar (yellow; bottom). How this was performed is explained in our previous work<sup>2</sup>. No scaling factor was applied to the normal mode wavenumbers.

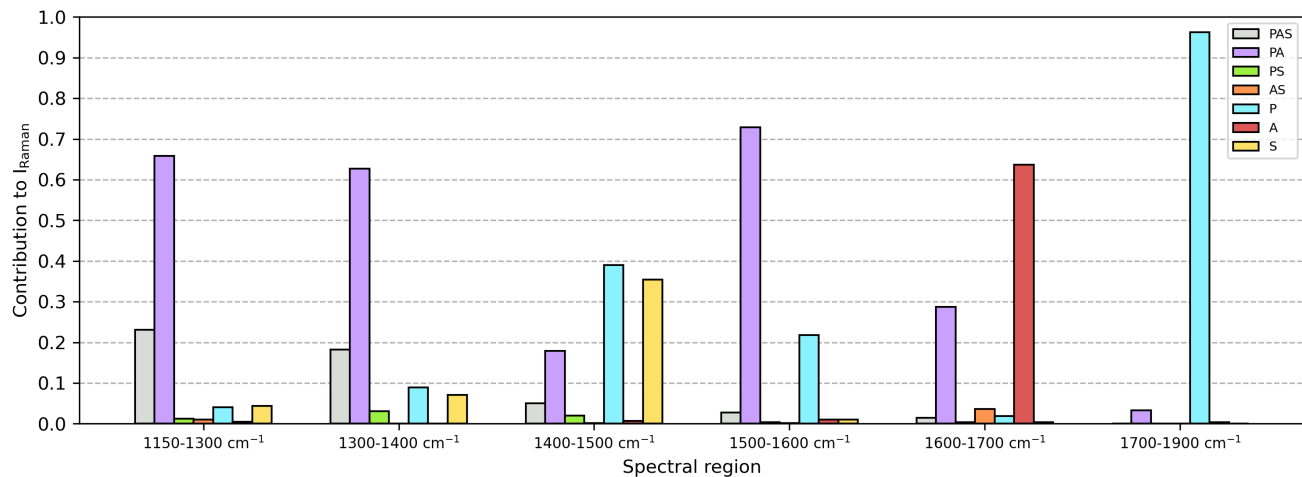


**Fig. S21** A bar graph to visualize the contributions of the normal modes – assigned to the peptide (P), sugar (S) and aromatic (A) entities, or any combination thereof (PAS, PA, PS, AS) – to the total Raman intensity in the specified spectral regions. The underlying normal modes and their assignment are presented in S17. The wavenumbers have not been scaled during this analysis.

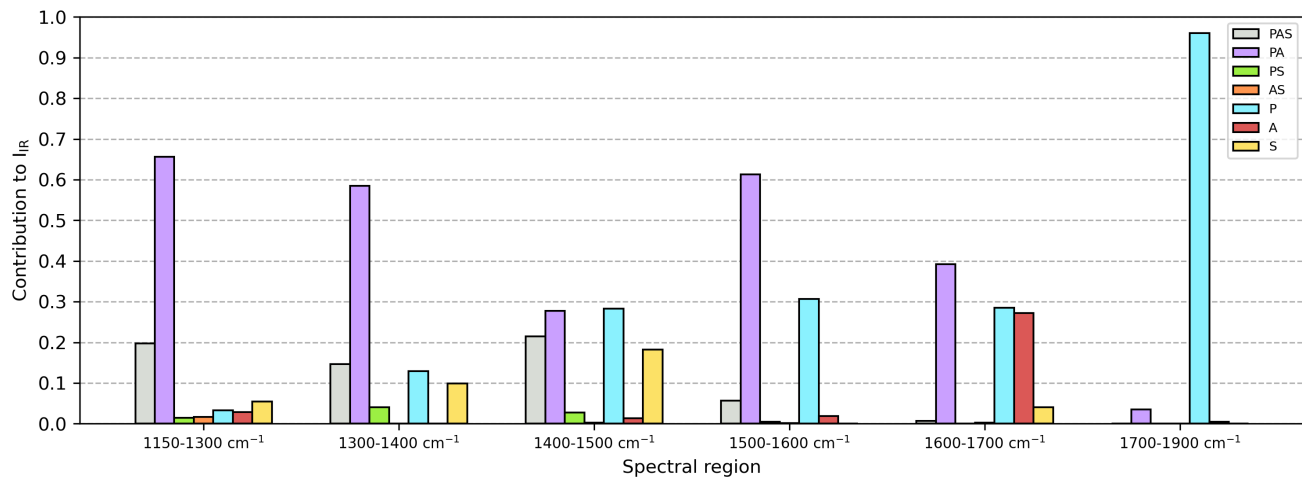


**Fig. S22** A bar graph to visualize the contributions of the normal modes – assigned to the peptide (P), sugar (S) and aromatic (A) entities, or any combination thereof (PAS, PA, PS, AS) – to the total IR intensity in the specified spectral regions. The underlying normal modes and their assignment are presented in S18. The wavenumbers have not been scaled during this analysis.

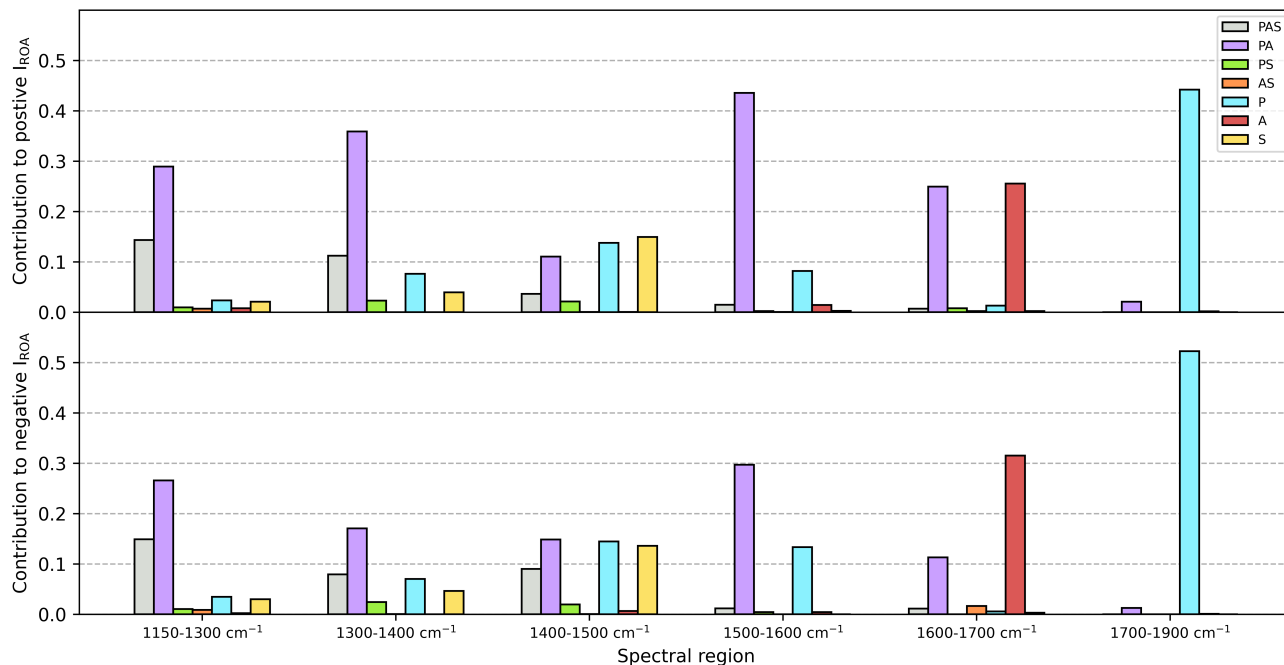


**Fig. S23** A bar graph to visualize the contributions of the normal modes – assigned to the peptide (P), sugar (S) and aromatic (A) entities, or any combination thereof (PAS, PA, PS, AS) – to the total Raman optical activity (ROA) intensity in the specified spectral regions. The contribution is split up for positive (top) and negative (bottom) intensities, but the percentage is always calculated with respect to the total (positive plus negative) ROA intensity in that spectral region. The underlying normal modes and their assignment are presented in S19. The wavenumbers have not been scaled during this analysis.

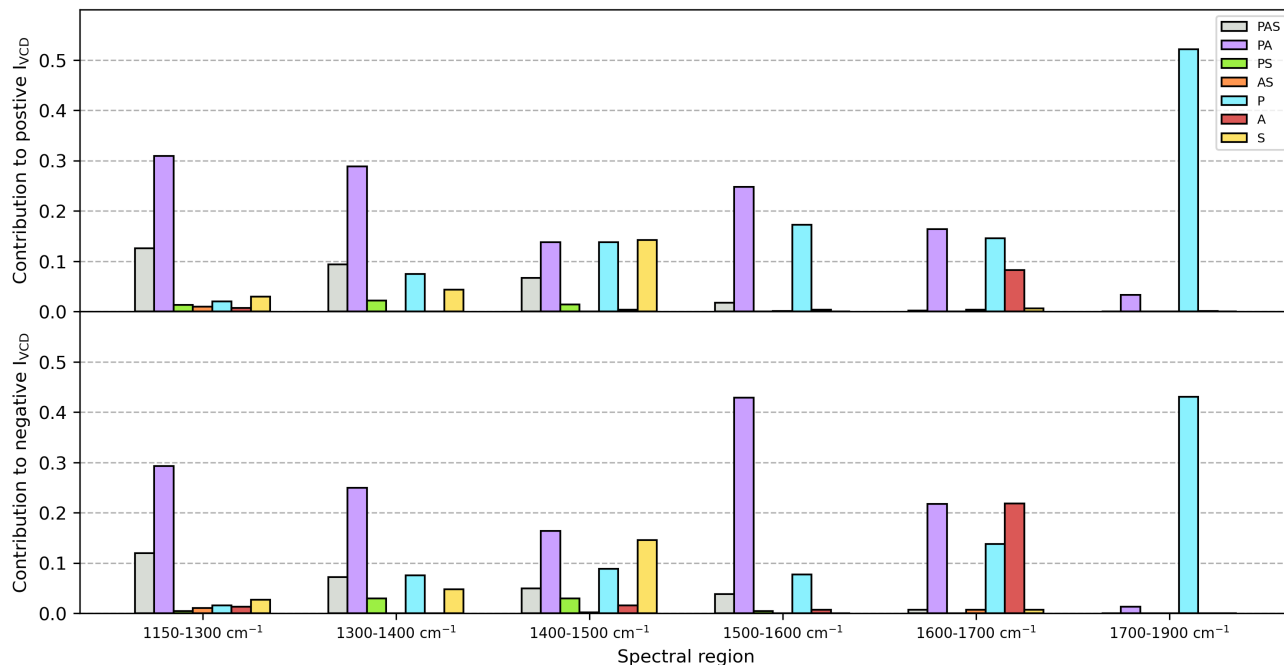


**Fig. S24** A bar graph to visualize the contributions of the normal modes – assigned to the peptide (P), sugar (S) and aromatic (A) entities, or any combination thereof (PAS, PA, PS, AS) – to the total vibrational circular dichroism (VCD) intensity in the specified spectral regions. The contribution is split up for positive (top) and negative (bottom) intensities, but the percentage is always calculated with respect to the total (positive plus negative) VCD intensity in that spectral region. The underlying normal modes and their assignment are presented in [S20](#). The wavenumbers have not been scaled during this analysis.

## S7 Spectral effects of carbohydrate entities

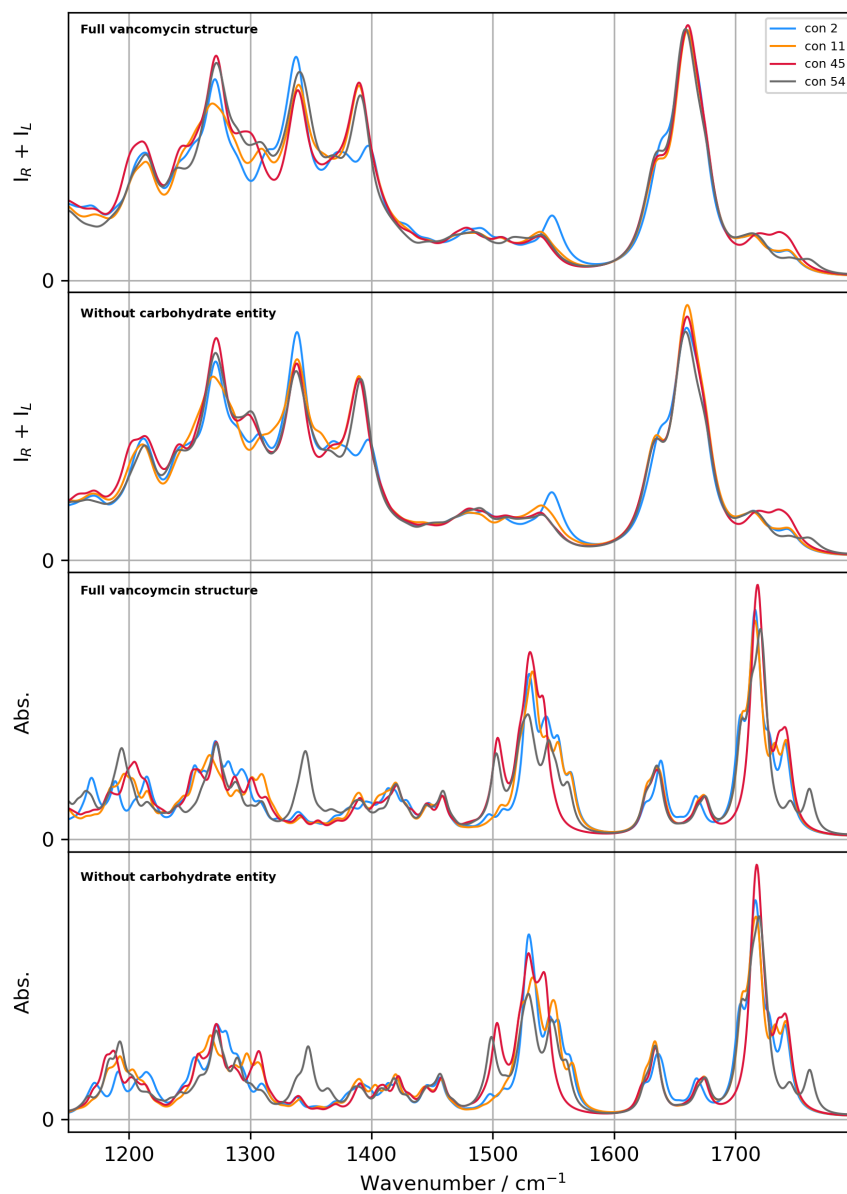


**Fig. S25** The calculated Raman (two top) and IR (two bottom) of vancomycin with and without the carbohydrate entity. This was done for four conformations, specified in the legend. The spectral overlap integrals between the system with and without the carbohydrate are given in Tabel S3.

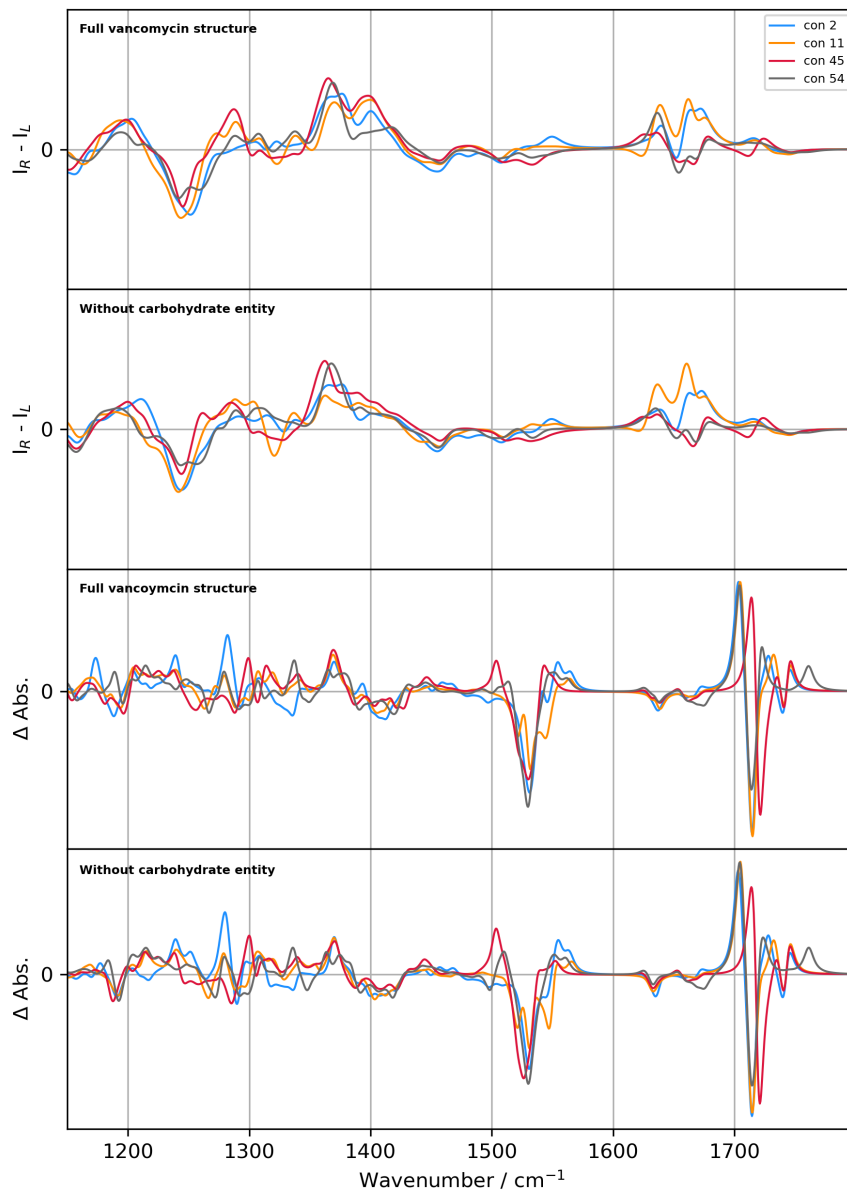


**Fig. S26** The calculated ROA (two top) and VCD (two bottom) of vancomycin with and without the carbohydrate entity. This was done for four conformations, specified in the legend. The spectral overlap integrals between the system with and without the carbohydrate are given in Tabel S3.

**Table S3** The overlap integrals between the calculated spectra of four selected conformations (see main text), visually presented in Fig. S25 and S26.

<b>Conformation</b>	<b>IR</b>	<b>Raman</b>	<b>VCD</b>	<b>ROA</b>
<b>2</b>	0.99	1.00	0.96	0.94
<b>11</b>	0.99	1.00	0.98	0.92
<b>45</b>	0.99	1.00	0.95	0.94
<b>54</b>	0.99	1.00	0.97	0.92



## S8 Spectral calculations of reoriented hydroxyl groups

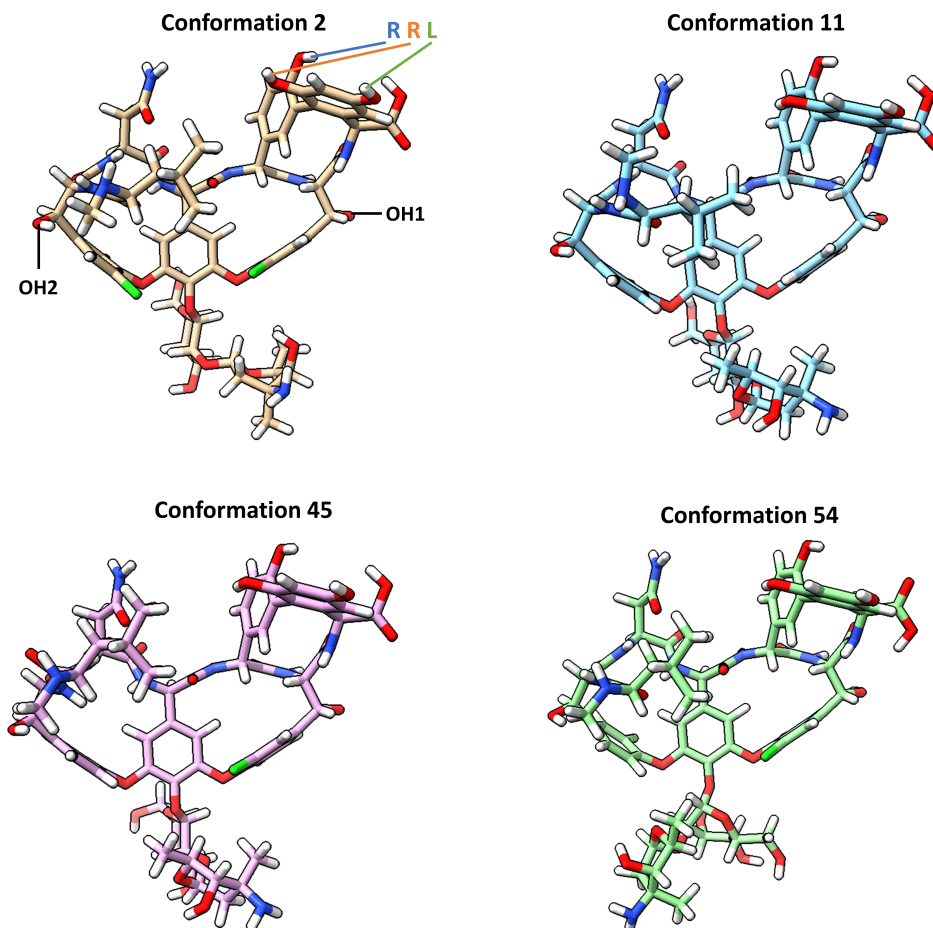


**Fig. S27** A visualization of conformations 2, 11, 45, and 54. For conformation 2 are indicated how the labels are used to indicate the hydroxyl orientation.

The original conformations 2, 11, 45, and 54 are depicted in Fig. S27. From these conformations, all different conformations where the hydroxyl groups (the five indicated in Fig. S27) were (simultaneously) reoriented were made for spectral calculations in order to investigate the spectral effect thereof with respect to the original conformation. The label **R** and **L** refer to the directionality of the hydroxyl group from the point of view indicated in Fig. S27, that is, pointing to the right and left, respectively. As such, the original orientations of conformation 2 is RRL, whereas those of conformation 11, 45, and 54 is RLL. The labels **OH1** and **OH2** refer to the opposite orientation of the respective hydroxyl groups. For each of the four conformations the OH1 group is pointing to the back and the OH2 group to the front. For the calculations, the label OH1 signifies that the OH1 group is pointing to the front. Similarly, the label OH2 indicates that this hydroxyl group is pointing to the back.

**Table S4** The overlap integrals between the calculated spectra of the original conformation and the calculated spectra of the hydroxyl reoriented conformations (spectral region 1150-1600  $\text{cm}^{-1}$ ). See Fig. S27 for the interpretation of the hydroxyl orientation labels.

Conformation	OH orientation	IR	Raman	VCD	ROA
2	lll	0.99	0.97	0.86	0.91
2	llr	0.98	0.97	0.78	0.89
2	lrl	0.99	0.98	0.86	0.96
2	lrr	0.99	0.97	0.82	0.94
2	oh1	0.98	0.99	0.90	0.96
2	oh2	0.98	1.00	0.96	0.97
2	rll	0.98	0.99	0.82	0.96
2	rlr	0.99	0.99	0.77	0.95
2	rrr	0.99	1.00	0.88	0.99
11	lll	0.99	0.98	0.83	0.98
11	llr	0.97	0.98	0.74	0.95
11	lrl	0.98	0.98	0.67	0.96
11	lrr	0.98	0.97	0.65	0.94
11	oh1	0.99	1.00	0.96	0.94
11	oh2	0.99	1.00	0.95	0.96
11	rlr	0.99	0.99	0.86	0.98
11	rll	0.99	0.99	0.83	0.96
11	rrr	0.99	0.98	0.77	0.95
45	lll	0.99	0.99	0.90	0.98
45	llr	0.98	0.98	0.85	0.97
45	lrl	0.98	0.98	0.73	0.96
45	lrr	0.99	0.97	0.73	0.95
45	oh1	0.99	1.00	0.92	0.94
45	oh2	1.00	1.00	0.87	0.97
45	rlr	0.99	0.99	0.91	0.99
45	rll	0.99	0.99	0.86	0.96
45	rrr	0.99	0.99	0.84	0.95
54	lll	0.99	0.99	0.89	0.95
54	llr	0.97	0.98	0.86	0.92
54	lrl	0.99	0.98	0.84	0.94
54	lrr	0.99	0.98	0.84	0.91
54	oh1	0.99	0.99	0.94	0.95
54	oh2	0.99	1.00	0.95	0.94
54	rlr	0.98	1.00	0.92	0.97
54	rll	0.99	0.99	0.90	0.95
54	rrr	0.99	0.99	0.85	0.94

## S9 Explicit DMSO spectral calculations

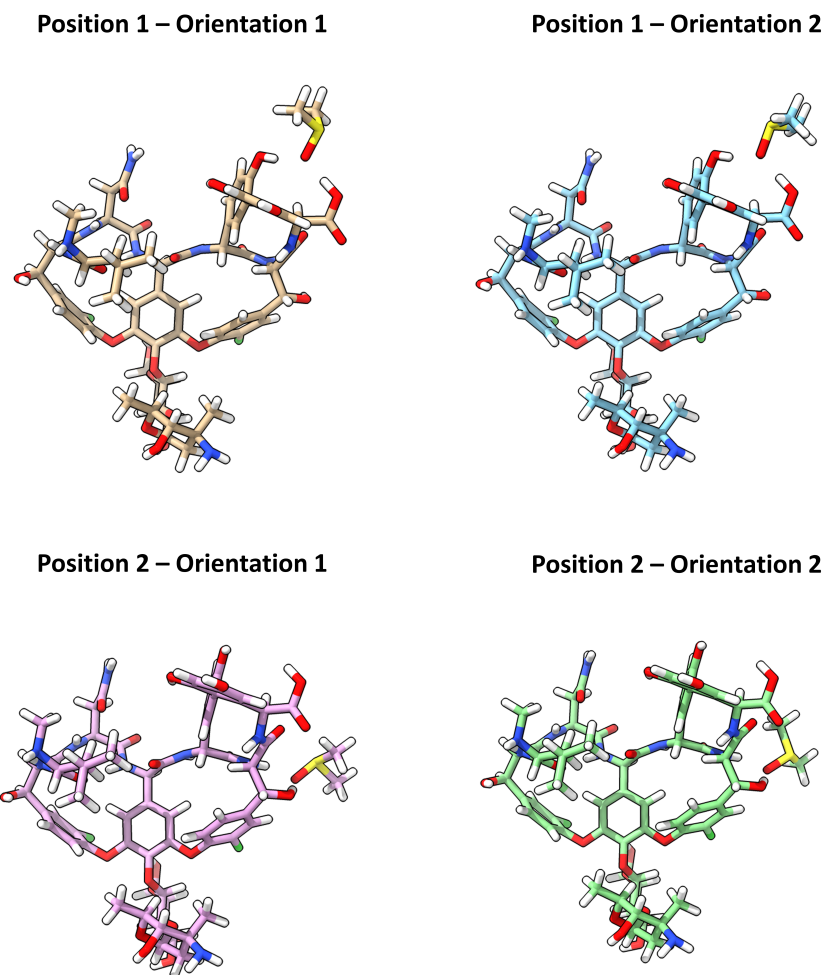


**Fig. S28** Visualizations of the geometrically optimized structures of DMSO-monosolvated vancomycin that were used for the spectral calculations. In this figure the optimized structures of conformation 11 with the explicit DMSO molecule is used.

To investigate the effect of explicit DMSO-solute interactions on the spectral calculations, four different input geometries were generated for each of the four conformations 2, 11, 45, and 54: two that form a hydrogen bond with the hydroxyl on the aromatic ring D (position 1) and two that form a hydrogen bond with the hydroxyl situated between bonds 20 and 21 (position 2; see Fig. S2 for labels). Two orientations were used, as visualized in Fig. S28. The spectral calculations were performed after a geometry optimization (the level of theory was B3PW91/6-31++G(d,p)). The overlap integrals of the final spectra with the original spectra (where DMSO was not taken into account explicitly) are given in Table S5.

**Table S5** The overlap integral values of the spectra of the four geometries presented in Fig. S28 with the original spectra, where no explicit solvent was considered (spectral region 1150-1600  $\text{cm}^{-1}$ ).

Conformation	Position - Orientation	IR	Raman	VCD	ROA
2	1 - 1	0.95	0.97	0.80	0.92
2	1 - 2	0.96	0.97	0.80	0.90
2	2 - 1	0.97	0.99	0.90	0.93
2	2 - 2	0.98	1.00	0.90	0.94
11	1 - 1	0.97	0.99	0.85	0.94
11	1 - 2	0.96	0.99	0.85	0.94
11	2 - 1	0.97	1.00	0.88	0.95
11	2 - 2	0.97	1.00	0.87	0.94
45	1 - 1	0.97	0.99	0.87	0.96
45	1 - 2	0.97	0.99	0.87	0.96
45	2 - 1	0.97	1.00	0.83	0.93
45	2 - 2	0.97	1.00	0.79	0.93
54	1 - 1	0.97	0.99	0.93	0.92
54	1 - 2	0.98	0.99	0.93	0.93
54	2 - 1	0.97	1.00	0.91	0.91
54	2 - 2	0.98	1.00	0.91	0.91

## References

- [1] H. F. Boelens, R. J. Dijkstra, P. H. Eilers, F. Fitzpatrick and J. A. Westerhuis, *Journal of chromatography A*, 2004, **1057**, 21–30.
- [2] R. Aerts, J. Vanhove, W. Herrebout and C. Johannessen, *Chemical Science*, 2021, **12**, 5952–5964.
- [3] S. G. Grdadolnik, P. Pristovšek and D. F. Mierke, *Journal of medicinal chemistry*, 1998, **41**, 2090–2099.
- [4] W. G. Prowse, A. D. Kline, M. A. Skelton and R. J. Loncharich, *Biochemistry*, 1995, **34**, 9632–9644.
- [5] C. Mensch, L. D. Barron and C. Johannessen, *Physical Chemistry Chemical Physics*, 2016, **18**, 31757–31768.
- [6] J. Bogaerts, F. Desmet, R. Aerts, P. Bultinck, W. Herrebout and C. Johannessen, *Physical Chemistry Chemical Physics*, 2020, **22**, 18014–18024.